ARMY RESEARCH LABORATORY

Mechanical and Electrochemical Performance of Graphene-Based Flexible Supercapacitors

by Matthew H Ervin, Linh T Le, and Woo Y Lee

ARL-TR-7042 **August 2014**

NOTICES

Disclaimers

The findings in this report are not to be construed as an official Department of the Army position unless so designated by other authorized documents.

Citation of manufacturer's or trade names does not constitute an official endorsement or approval of the use thereof.

Destroy this report when it is no longer needed. Do not return it to the originator.

Army Research Laboratory
Adelphi, MD 20783-1138

ARL-TR-7042 **August 2014**

Mechanical and Electrochemical Performance of Graphene-Based Flexible Supercapacitors

Matthew H Ervin
Sensors and Electron Devices Directorate, ARL

Linh T Le and Woo Y Lee
Department of Chemical Engineering and Materials Science
Stevens Institute of Technology

REPORT DOCUMENTATION PAGE	Form Approved OMB No. 0704-0188

1. REPORT DATE *(DD-MM-YYYY)*	2. REPORT TYPE	3. DATES COVERED (From - To)
August 2014	Final	October 2013 to August 2014

4. TITLE AND SUBTITLE
Mechanical and Electrochemical Performance of Graphene-Based Flexible Supercapacitors

5a. CONTRACT NUMBER

5b. GRANT NUMBER

5c. PROGRAM ELEMENT NUMBER

6. AUTHOR(S)
Matthew H Ervin, Linh T Le, and Woo Y Lee

5d. PROJECT NUMBER

5e. TASK NUMBER

5f. WORK UNIT NUMBER

7. PERFORMING ORGANIZATION NAME(S) AND ADDRESS(ES)
U.S. Army Research Laboratory
ATTN: RDRL-SER-L
2800 Powder Mill Road
Adelphi, MD 20783-1138

8. PERFORMING ORGANIZATION REPORT NUMBER
ARL-TR-7042

9. SPONSORING/MONITORING AGENCY NAME(S) AND ADDRESS(ES)

10. SPONSOR/MONITOR'S ACRONYM(S)

11. SPONSOR/MONITOR'S REPORT NUMBER(S)

12. DISTRIBUTION/AVAILABILITY STATEMENT
Approved for public release; distribution unlimited.

13. SUPPLEMENTARY NOTES

14. ABSTRACT
Flexible supercapacitors are being developed for powering flexible electronics for military and commercial applications. Graphene oxide dispersed in water has been used for inkjet printing the active electrode material onto metal film on Kapton current collectors. After printing, the graphene oxide was thermally reduced to produce conductive graphene electrodes. These electrodes were heat sealed together with added electrolyte and a polymer separator, and the resulting supercapacitor performance is good, with excellent capacitance retention with flexing demonstrated. A number of issues associated with using Kapton for packaging these devices have also been investigated.

15. SUBJECT TERMS
Supercapacitor, electrochemical capacitor, graphene, inkjet printed, graphene oxide

16. SECURITY CLASSIFICATION OF:			17. LIMITATION OF ABSTRACT	18. NUMBER OF PAGES	19a. NAME OF RESPONSIBLE PERSON
A. Report	b. ABSTRACT	c. THIS PAGE			Matthew H Ervin
Unclassified	Unclassified	Unclassified	UU	26	19b. TELEPHONE NUMBER (*Include area code*) (301) 394-0017

Standard Form 298 (Rev. 8/98)
Prescribed by ANSI Std. Z39.18

Contents

List of Figures

List of Tables

INTENTIONALLY LEFT BLANK.

1. Background

Printed, flexible electronics are desirable as they offer the promise of low-cost, readily customizable, rugged, and perhaps, wearable electronics along with volume and weight savings. In order to fully realize these advantages, a flexible power source must be developed. Presently, batteries are the go-to solution for powering most portable commercial and military electronics; however, there are good reasons for considering the use of electrochemical double-layer capacitors (commonly referred to as "supercapacitors") for high power charging/discharging and long cyclic life applications. While batteries have superior energy densities, supercapacitors have advantages in power density, cycle life, and shelf life, and exhibit rapid charging/discharging and good performance over a wide temperature range.[1] Supercapacitors may prove useful as a standalone power source or as part of a hybrid system with a battery, depending on the application. Here we report on inkjet-printed, graphene-based supercapacitors that are flexible and conformal. These supercapacitors can be placed onto a cylindrical-shaped object for systems that have severe size and weight constraints or those for which flexible electronics would otherwise provide a benefit. Inkjet printing has the benefits of 50-µm resolution, additive, net-shape manufacturing with minimal nanomaterial use/waste generation, and a scale-up capability for integration with rapidly emerging printed electronics.[2]

Commercial supercapacitors have electrodes made with activated carbon. Activated carbon has high surface area, which yields high specific capacitances, but it is composed of brittle particles that are not highly conductive. As a result, activated carbon electrodes are made with the addition of binders and conductivity enhancers. On the other hand, graphene, single-atom-thick graphite sheets, has superior electrical and mechanical properties compared to activated carbon. Graphene is being widely studied for supercapacitor applications due to its high surface area and high electrical conductivity.[3] Graphene-based materials are especially attractive for printing flexible supercapacitors as graphene is a very strong and flexible material, and its oxidized form (graphene oxide [GO]) makes a good inkjet printable ink when dissolved in water. Once GO is printed onto the substrate, it must be reduced to the conductive graphene form, which we do with a thermal anneal.

Previously, we reported good capacitor performance with inkjet-printed graphene on metal foil current collectors, which were assembled into a prototype device using a Celgard 3501 separator and a rigid fluoropolymer clamp, as shown in Fig. 1a.[4] The achieved specific capacitance is similar to that obtained for graphene using other electrode fabrication methods. This demonstrates that inkjet printing is a viable method of electrode fabrication. Figure 2 shows a cross-sectional scanning electron microscopy (SEM) image of graphene inkjet-printed onto a silicon wafer, which was then cleaved to show the internal structure of the graphene electrodes.

The graphene was observed to be deposited as stacks of quasi-parallel sheets that have intervening spaces, which allow access for the electrolyte.

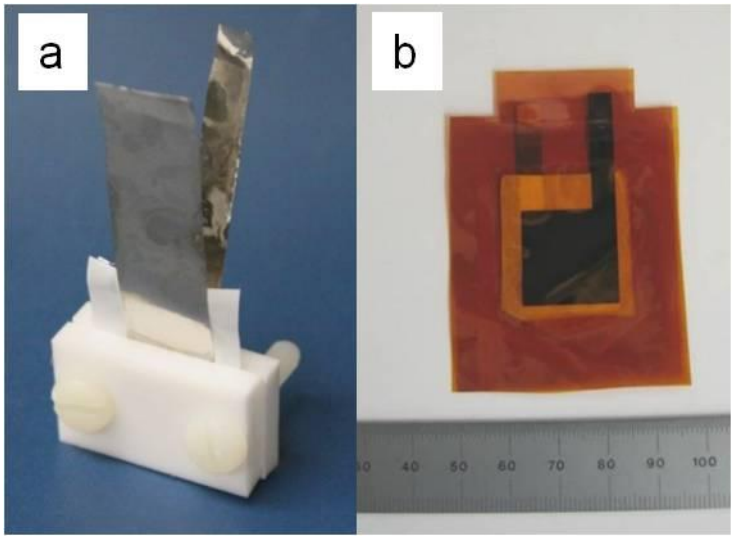

Fig. 1 Pictures of inkjet-printed supercapacitor prototypes: a) inkjet-printed graphene on metal foil current collectors tested in a rigid clamp and b) heat sealed device made with inkjet-printed graphene and evaporated metal on Kapton current collectors

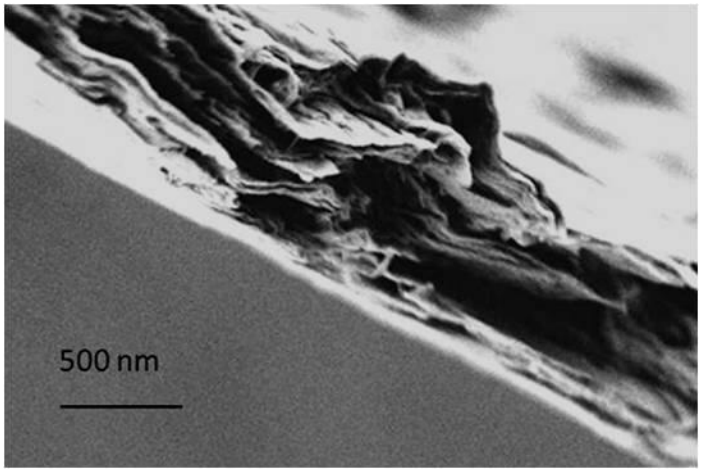

Fig. 2 Cross-sectional SEM image of inkjet-printed graphene on a silicon wafer

In this work, the next step in printing flexible supercapacitors was undertaken with the printing of graphene electrodes onto flexible Kapton films, which were composed of polyimide with or without fluorinated ethylene propylene (FEP) coatings. Kapton was chosen as the substrate as it is frequently used as a substrate for flexible electronic circuits due to its good dielectric properties, low outgassing, and thermal stability. Kapton is stable to 400 °C, which will be an advantage when more of the supercapacitor components are printed. For example, it will facilitate the printing of metal current collectors by printing metallic nanoparticles such as gold

(Au) and sintering the nanoparticles at temperatures above 200 °C. The thermoplastic FEP coating is what allows the Kapton to be heat sealed, since the Kapton itself thermally decomposes before melting. A prototype graphene/Kapton supercapacitor is shown in Fig. 1b. The compatibility of the Kapton packaging was also tested for use with various common electrolytes.

2. Experimental

While it is expected that eventually the metal current collector, graphene active electrode material (with or without binder), and perhaps, the electrolyte and separator will all be inkjet-printed, in this initial prototype, the metal current collectors were shadow-masked metal films evaporated onto Kapton. Evaporated metal films were used here, as currently there are few metal inks developed for inkjet printing. The most widely available and proven metal ink is silver, which we found to be electrochemically unstable in the electrolytes we were using. More metal ink development is required to obtain low resistivity and electrochemically resistant inkjet-printed current collectors.

The evaporated current collectors are 2 x 2 cm with a lead, and the graphene is printed on them in a 1 x 1 cm square, as can be seen in Fig. 3a. The Kapton was obtained from American Durafilm with and without an FEP coating. The current collectors used consisted of 50-nm titanium (Ti)/300-nm platinum (Pt), or 20-nm Ti/230-nm Au films electron-beam evaporated onto FEP-coated Kapton or bare Kapton films. The GO was printed onto these current collectors using a Dimatix Material Printer DMP 2800 inkjet printer.

The GO ink is a 2-mg/ml GO solution in water obtained from Cheap Tubes, Inc, and it was sonicated for 15 min and filtered through a 450-nm syringe filter before loading into the printhead.[4] Owing to the low concentration of the GO ink, multiple print passes were made to obtain the desired electrode mass. Once printed, the electrodes were annealed at 225 °C for 4 h to reduce the GO to conductive graphene. The resulting reduced graphene oxide (rGO) electrodes had 0.1 to 0.37 mg/cm^2 of rGO as determined by weighing similar printings made on silicon wafers. Attempting thicker electrodes resulted in rGO delamination due to shrinkage as the film dries, indicating that a binder may be required to make thicker electrodes.

The reduced electrodes were then assembled into supercapacitors, as shown in Fig. 3. The first step was to heat seal three sides of the supercapacitor with the printed electrodes face to face. Heat sealing was done using a Packworld PW7016 HT heat sealer at 375 °C for 60 s. This could be done directly when using single-side FEP-coated Kapton (200FN011, 51-μm Kapton with 51-μm FEP), or it required an intervening frame of double-side FEP-coated Kapton (300FN929, 51-μm Kapton with 12.7-μm FEP on both sides) when using plain Kapton (HN200, 51-μm Kapton). An electrode separator of Celgard 3501 is then inserted between the electrodes, 50 μl of

electrolyte is injected, and then the last seal is made while minimizing the amount of trapped air in the device. Various electrolytes were used in this work including 0.5 M potassium sulfate (K_2SO_4), 1 M sulfuric acid (H_2SO_4) (Sigma Aldrich), and the ionic liquid: 1-butyl-3-methylimidazolium tetrafluoroborate (BMIM BF_4) (Strem Chemicals). When BMIM BF_4 was used, the electrodes and electrolyte were dried in a vacuum oven prior to assembling the device in a dryroom to prevent inclusion of water, which would reduce the operating voltage of the device.

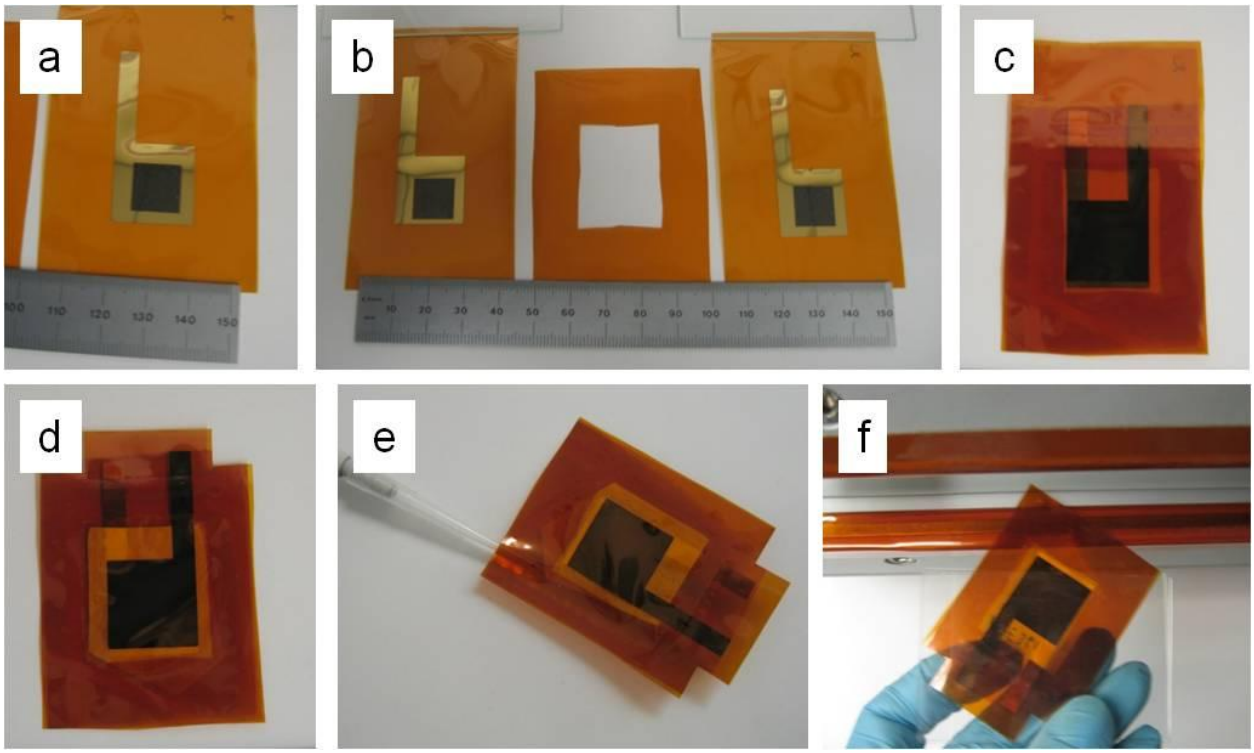

Fig. 3 Flexible supercapacitor assembly process: a) GO printed on a metal current collector on Kapton and reduced at 200 °C, b) two electrodes are assembled with an intervening frame of FEP-coated Kapton, c) electrodes are heat sealed face to face on three sides, d) the polypropylene separator is put between the electrodes, e) the electrolyte is added, and f) the final seal is made

The supercapacitors were tested using cyclic voltammetry (CV) from 0–1 V for the aqueous electrolytes and 0–3 V for BMIM BF_4, electrochemical impedance spectroscopy from 100 kHz to 1 mHz at 0 V, and charge/discharge testing from 0–1 V (aqueous) or 0–3 V (BMIM BF_4) at 0.01–10 A/g. Each current in the charge/discharge testing was repeated to verify reproducibility. For the Kapton permeability experiments, various electrolyte solvents were sealed in different types of Kapton and the masses of the sealed pouches were monitored using a Mettler Toledo XP 26 balance. The acetonitrile and propylene carbonate solvents were obtained from Sigma Aldrich, and an ionic liquid, 1,2-dimethyl-3-propylimidazolium bis(trifluoromethysulfonyl)imide, was obtained from Iolitec Inc.

3. Results and Discussion

3.1 Supercapacitor Packaging

The first flexible supercapacitor prototype was made using evaporated Ti/Pt current collectors on FEP-coated Kapton. While printing on FEP-coated Kapton simplified the capacitor assembly, the FEP layer was found to be an unsuitable substrate. The Ti/Pt film was found to have cracks as deposited, perhaps due to thermal flow of the FEP during the electron-beam evaporation of the metal current collector. This resulted in a resistive current collector (~125 ohms end to end). Worse yet, when the heat seal across the current collector leads was made, the current collector film broke up, resulting in an open circuit. This can be seen in Fig. 4, and it was the result of the FEP flowing during the formation of the heat seal. As a result, it was determined that the current collector should be evaporated onto bare Kapton, with FEP-coated Kapton used to seal the devices.

Subsequent devices used evaporated Ti/Au on bare Kapton current collectors. These current collectors were continuous films of low resistance (~0.7 ohms end to end), and they remained intact through the heat sealing process. In the current devices, this required a frame of FEP-coated Kapton to seal the two electrodes together, but in the future, interdigitated devices could be printed on a bare Kapton substrate with a capping layer of FEP-coated Kapton being used to seal the device.

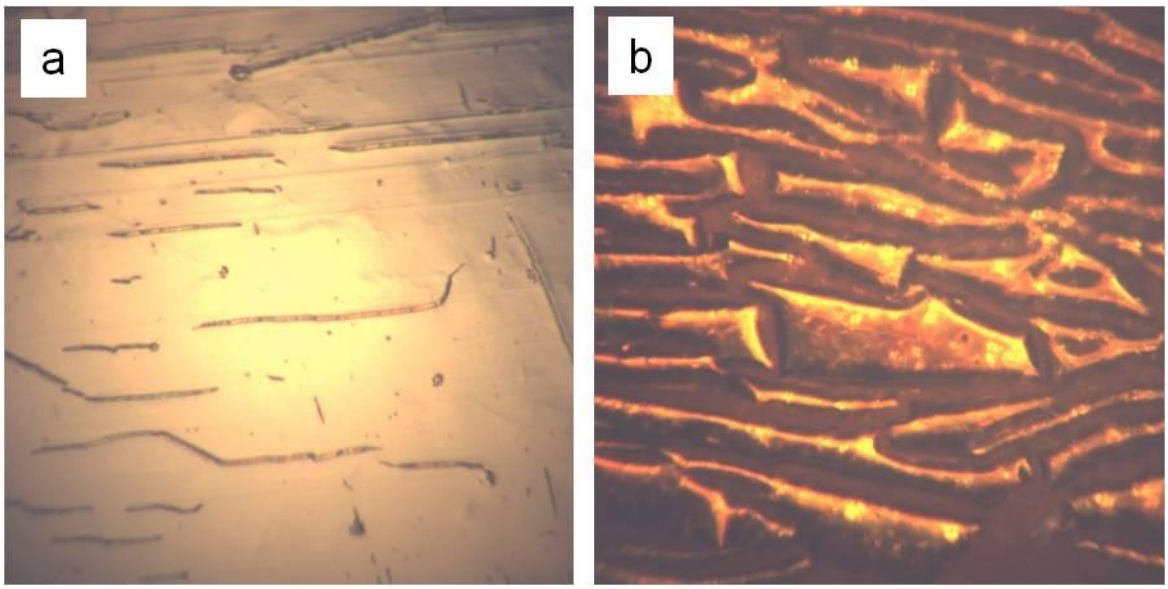

Fig. 4 Optical micrographs of the metal film current collector on FEP-coated Kapton during processing: a) the Ti/Pt current collector film on FEP-coated Kapton is cracked as deposited and b) becomes fully discontinuous where the heat seal is made. (These micrographs are 500 μm across.)

In this investigation, we have used Kapton-based materials to fabricate these supercapacitors. While Kapton and FEP have good chemical inertness, there are a number of reasons to suspect that they may not be good packaging materials. Kapton itself is permeable to water and oxygen, which may lead to electrolyte degradation. The FEP sealing layer is also permeable to small molecules, e.g., carbon dioxide (CO_2).[5] In addition, we found that FEP does not produce strong bonds with Kapton even if the Kapton is corona treated to enhance bonding. In the course of working with these prototype supercapacitors, it was found that the Kapton is not an adequate packaging material when using aqueous electrolytes. These devices, as is, would not have an adequate shelf life to be useful. Accordingly, an investigation into the permeability of the packaging materials was undertaken. Typical supercapacitor electrolyte solvents were sealed into pouches made of various Kapton thicknesses with and without FEP. The mass of these packaged solvents was then monitored gravimetrically to determine whether the solvent was evaporating through the packaging materials. The solvents tested were water, acetonitrile, propylene carbonate, and an ionic liquid. It was found, as can be seen in Fig. 5, that the FEP/Kapton was insufficient to contain the water, acetonitrile, or propylene carbonate. The acetonitrile was, in particular, difficult to contain, which is unfortunate since organic electrolytes have larger potential windows than aqueous electrolytes, and acetonitrile produces significantly more conductive electrolyte compared to propylene carbonate.[8]

However, the ionic liquid, being a larger molecule with a low vapor pressure, showed no significant mass loss during the experiment. In fact, its mass was stable even if the package was not sealed, owing to its low vapor pressure. Additional experiments will be required to determine if enough water diffuses into the ionic liquid electrolyte to degrade its performance. The evaporation of water was also significantly slowed if aluminum tape was applied to the package. This is not surprising, as metal layers are frequently used in hermetic packaging due to their impermeable nature.

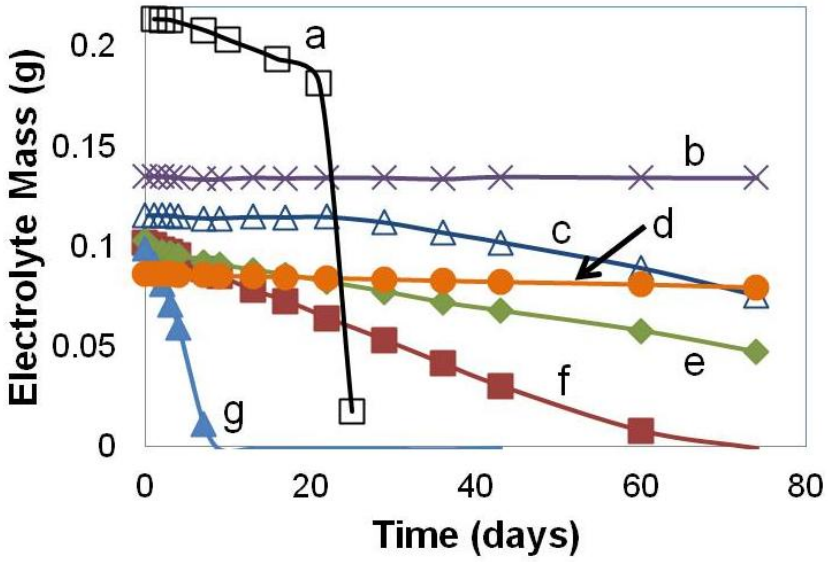

Fig. 5 Gravimetric measurement of electrolyte solvents loss through various packaging materials: a) acetonitrile in thick Kapton/FEP, b) ionic liquid in thick Kapton/FEP, c) propylene carbonate in thick Kapton, d) water in thick Kapton covered with aluminum tape, e) water in thick Kapton/FEP, f) water in thin Kapton/FEP, and g) water in thin Kapton

Future devices may require the use of flexible polymeric packaging materials that contain metal foil laminates for their hermetic properties. We have investigated one such material to determine if it is compatible with the typical supercapacitor electrolytes. This metal foil containing laminate (SP class PPD from Shield Pack Specialty Packaging, LLC) has been tested for compatibility with propylene carbonate, acetonitrile, 0.5 M K_2SO_4 in water, 1 M H_2SO_4, and 1 M potassium hydroxide (KOH). This material is a laminate of polyester, polyethylene, metal foil, and an ethylene/methacrylic acid copolymer heat sealing layer. An initial two-month test has shown it to be compatible with all of these electrolytes/solvents.

More standard pouch cell packaging materials, such as this one, also produce much better heat seal bond strengths as the Kapton/FEP bonds mechanically fail at fairly low forces due to delamination at the Kapton/FEP interface. This PPD material was found to have too low a thermal stability to allow for the thermal reduction of the printed GO. Therefore, another metal foil laminate material comprising polyester, aluminum foil, nylon, and a polypropylene heat sealing layer was also investigated. While this material has a higher thermal budget, which allowed at least minimal thermal reduction of the GO, it was found that it was very difficult to get it to form a bond to the metal tabs used to bridge gaps in the current collector leads. These tabs made it possible to maintain conductivity across the heat seal, but they made it difficult to get a hermetic seal with this packaging material. Therefore, there is still room to improve on the packaging materials used for these devices.

3.2 Supercapacitor Electrochemical Performance

The CV curve of one of these flexible reduced GO devices is shown in Fig. 6. The CV shows a good rectangular shape, indicating good double-layer capacitive behavior. A specific capacitance, based on the mass of graphene only, of 132 F/g was measured at 20 mV/s. This specific capacitance was calculated from the CV using Eq. 1:

$$C_{sp} = (i/\nu m) * 4 \quad (1)$$

where C_{sp} is the specific capacitance of the active electrode material (F/g), i is the average of the magnitudes of the oxidation and reduction currents (A) measured for the two-electrode cell at 0.5 V on the CV, ν is the scan rate (V/s), and m is the total mass (g) of graphene on both electrodes. The reported value is multiplied by four to report the results in the single electrode standard as would be measured with a three-electrode cell.[6] The capacitance was calculated as measured at the midpoint of the CV curve as it did not include any undue contribution from redox peaks and was therefore considered representative of the device.

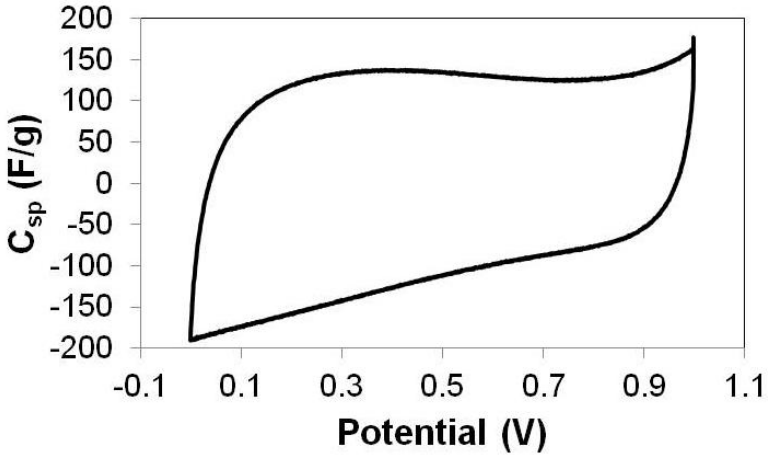

Fig. 6 CV of a packaged, flexible, graphene-based supercapacitor using 0.5 M K_2SO_4 electrolyte. The specific capacitance of the graphene electrode material has been plotted vs. the scan potential.

Electrochemical impedance spectroscopy shows that good capacitive performance can be achieved with these flexible supercapacitors. Figure 7 compares the phase angle of a flexible supercapacitor to that of a commercial supercapacitor. Both approach a phase angle of approximately –80° at low frequency. The flexible device maintains close to this phase angle up to approximately 1 Hz, which is much higher than the commercial device. This is because the flexible device has thinner electrodes, which have lower overall ionic/electronic impedance. Typically, thinner electrodes are faster than thicker electrodes while thicker electrodes are capable of storing more energy.

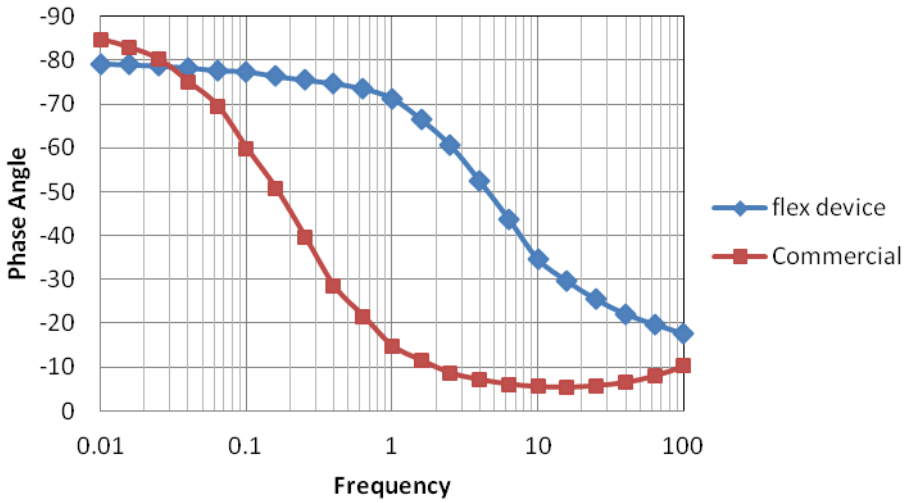

Fig. 7 Phase angle plots of flexible supercapacitor with H_2SO_4 and a commercial supercapacitor

The constant current testing of this device is shown in Fig. 8. Again, the linear charging and discharging indicates good capacitive behavior. Each current was run twice to verify reproducibility of the measurement on the device, with the second discharge at each current used for calculating the energy and power densities. The specific capacitance was calculated similarly to the CV case for each current tested from the constant current plots. The slope of the discharge curve is used to calculate a scan rate, ν, and the applied current is used for i in formula 1. The specific energy was then calculated using Eq. 2:[7]

$$Wh/kg = (C_{sp} * V^2_{max} / 8) / 3.6 \quad (2)$$

where the specific energy (Wh/kg) of the cell, based on the mass of graphene, is calculated using the specific capacitance (C_{sp} in F/g) of the electrode material and the maximum cell voltage (V_{max}, 1 V for an aqueous cell). The factor of 8 includes a factor of 4 for converting from a single electrode to a two-electrode device, and the factor of 3.6 converts from J/g to Wh/kg.

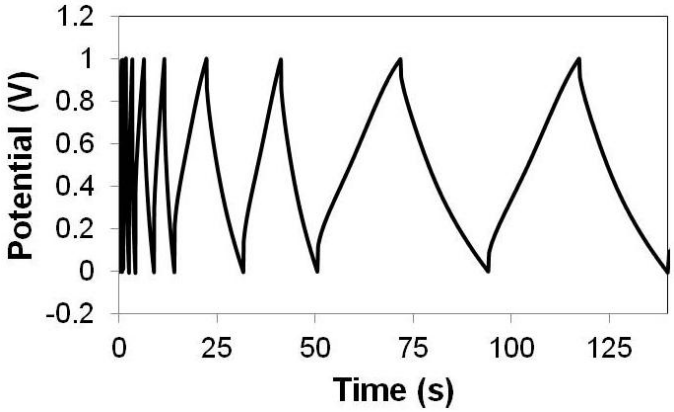

Fig. 8 Charge/discharge testing of a packaged, flexible, graphene-based supercapacitor using 0.5 M K_2SO_4 electrolyte

The power density was calculated using Eq. 3:

$$kW/kg = 0.5\ C\ (V^2_i - V^2_f) / (t * m) \quad (3)$$

where the specific power (kW/kg) of the cell, based on the mass of graphene, is calculated using the measured two-electrode capacitance (C in F), the initial voltage (V_i) after the equivalent series resistance (ESR) drop, the final voltage (V_f), the discharge time (t in seconds) from V_i to V_f, and the mass of graphene in the device (m in kg). The calculation is made based on a final voltage of half the initial voltage as discharging to half of the maximum voltage represents 75% of the stored energy being discharged, and it avoids counting energy that is only available at low voltages, which may not be useful.

The calculated performance of the inkjet-printed device (Table 1) included a specific capacitance of 132 F/g, an energy density of 2.55 Wh/kg measured at 1.1 A/g, and a power density of 5.78 kW/kg measured at 11 A/g using 0.5 M K_2SO_4 electrolyte. Similarly, we measured 192 F/g, 5 Wh/kg, and 10 kW/kg with 1 M H_2SO_4 electrolyte. When the ionic liquid BMIM BF_4 was used, the results were 73 F/g (at 20 mV/s), 5.5 Wh/kg (at 0.25A/g), and 19 kW/kg (at10 A/g), measured over 0–3V.

Table 1 Electrochemical performance with various electrolytes

	0.5 M K_2SO_4 0–1 V	**1M H_2SO_4 0–1 V**	**BMIMBF$_4$ 0–3 V**
Capacitance (F/g)	132 at 20 mV/s	192 at 20 mV/s	73 at 20 mV/s
Energy Density (Wh/kg)	2.6 at 1.1 A/g	5.0 at 0.25 A/g	5.5 at 0.25 A/g
Power Density (kW/kg)	5.8 at 11 A/g	10 at 10 A/g	19 at 10 A/g

The energy and power densities above were calculated as a function of graphene mass only. In the end, it will be the specific energy and power densities of the entire device that will be important. These prototypes are far from optimized in that regard. In particular, we have made ~3 x 3 cm devices containing ~1 cm^2 active electrode areas. A 6.9-mF capacitor of 0.24 g with BMIM BF_4 electrolyte was demonstrated. A Ragone plot showing the energy and power densities of devices as a function of rGO mass and of full package mass is shown in Fig. 9. For comparison, information on a commercial lithium (Li)-ion battery is also shown. While people frequently estimate that dividing the energy and power densities by a factor of three is sufficient to estimate the packaged specific densities, this is clearly not the case for our devices. However, to obtain the flexible characteristics for our devices, we have made essentially two-dimensional devices. As a result, the surface area to volume of the devices is very large compare to a three-dimensional device such a coin cell or cylindrical can device. This results in a much higher

proportion of packaging materials in the device, so there are potentially significant energy and power density penalties associated with the flat, flexible device form factor. While packaged specific performance was low, there are a number of opportunities to optimize it. There is excessive packaging material, separator, electrolyte, etc., which would need to be reduced/optimized for the final device. In addition, the thicknesses of the graphene electrodes would have to be optimized for the total device performance, which will require thicker electrodes, which may require the use of a binder to prevent electrode flaking.

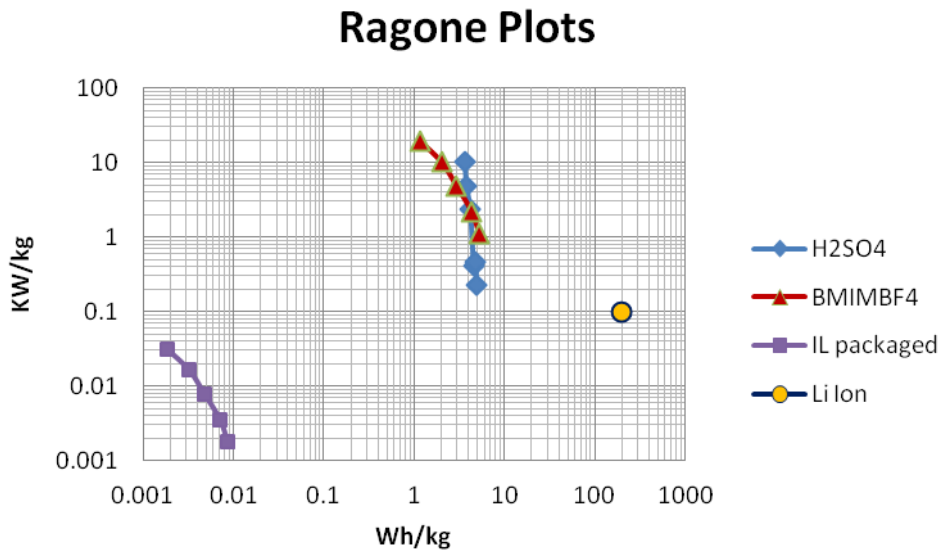

Fig. 9 Ragone plot of flexible supercapacitors and a commercial coin cell supercapacitor and Li-ion battery

The electrical cycle lives of these flexible devices were also characterized. It was found that a flexible device annealed at 140 °C for 16 h had a capacitance that degraded with cycling, as shown in Fig. 10. In order to investigate this further, coin cells were made varying various parameters such as using a binder or no binder, annealing at different temperatures, and comparing to chemically reduced GO or electrochemically exfoliated graphene, which is not oxidized to begin with. It was found that the binder did not improve the life cycle performance indicating that it is not a mechanical degradation of the electrodes reducing the capacitance. The low temperature (140 °C) and chemically reduced graphene also deteriorated with cycling. Also, while the electrochemically exfoliated graphene did actually improve with cycling, its capacitance was significantly lower than for the high temperature (225 °C, 4 h) annealed GO, which showed the best capacitance and an initially increasing capacitance, perhaps due to electrowetting during the initial cycling. Figure 11 shows the capacitance of the 140 °C, 16 h and 225 °C, 4 h annealed coin cells normalized to their respective 1st cycle capacitances. In absolute terms the 140 °C annealed device goes from 89 to 67 F/g with cycling, while the 225 °C annealed device goes from 104–124 F/g with cycling. Apparently, a more rigorous thermal reduction improved the capacitance and lifecycle stability of the devices.

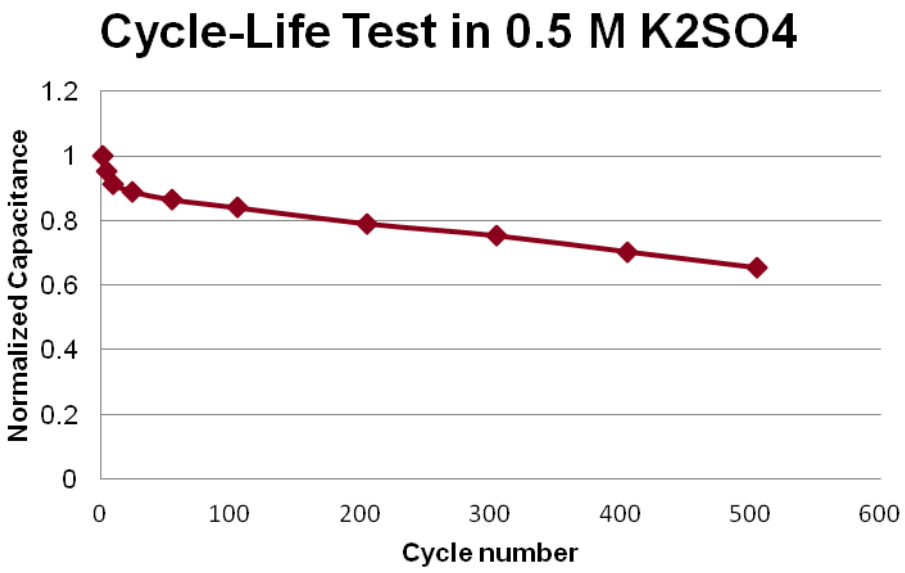

Fig. 10 Normalized capacitance as a function of cycling the device with 0.5 M K_2SO_4 electrolyte

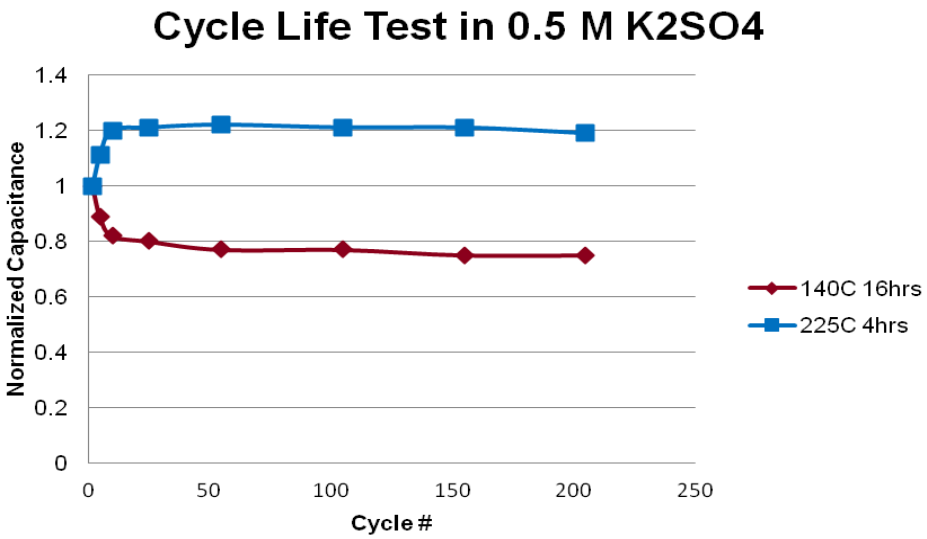

Fig. 11 Normalized capacitance of a device annealed at 140 °C for 16 h and one annealed at 225 °C for 4 h

3.3 Supercapacitor Flexing Performance

The purpose of this work was to demonstrate a flexible, inkjet-printed, graphene-based supercapacitor, and so the capacitance was measured as the capacitor was bent to different radii. Figure 12 shows that the capacitance dropped by only 3% as the capacitor was bent through radii of ∞, 65 mm, 40.5 mm, 34.1 mm, 25.0 mm, 14.5 mm, and back to ∞ (unbent). It was noticed, however, that in order to obtain consistent capacitance measurements, the capacitor electrodes needed to be pressed together so that bending-induced wrinkling did not pull them apart reducing the measured capacitance. This problem is reduced when using thinner Kapton films. An

interdigitated electrode approach would eliminate this issue, and the use of a gel electrolyte may also hold the electrodes together during bending.

The effect of multiple flexing cycles was also measured. Figure 13 shows the capacitance change as the result of 250 cycles of bending to an 8.25-mm radius, while Fig. 14 shows the same device subsequently bent 100 times to a 4-mm radius. There is a total of 5% capacitance loss through the entire 350 cycles of bending, which shows very good capacitance retention with bending.

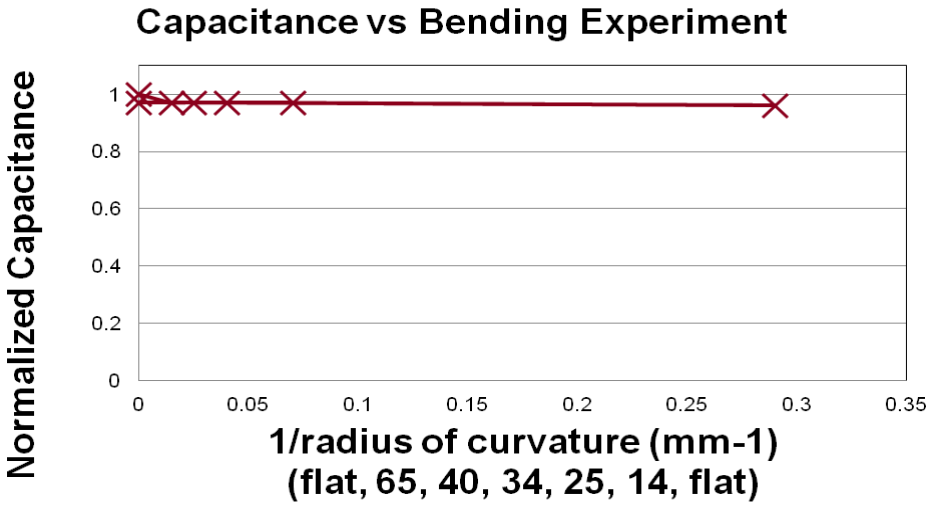

Fig. 12 Capacitance measured as the 0.5 M K_2SO_4 electrolyte containing supercapacitor is bent to different radii of curvature, with the first and last measurements made with a flat capacitor

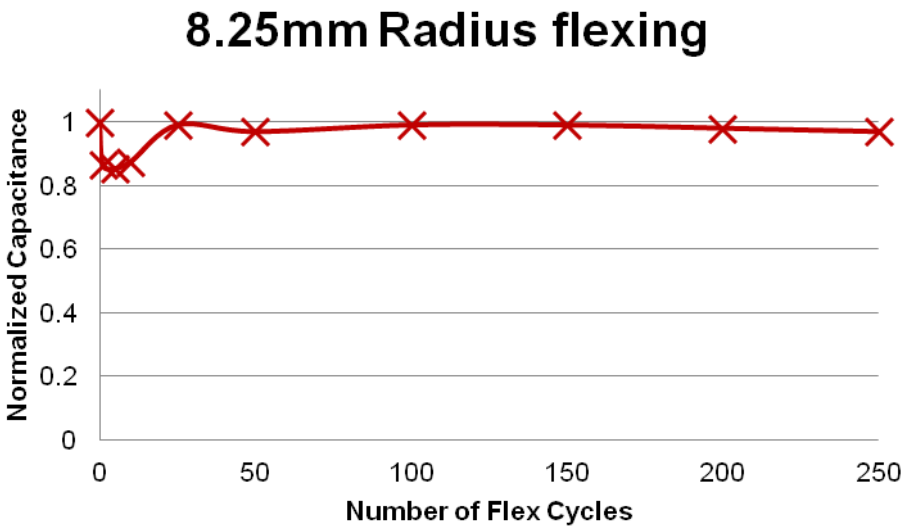

Fig. 13 Normalized capacitance after repeated capacitor flexing

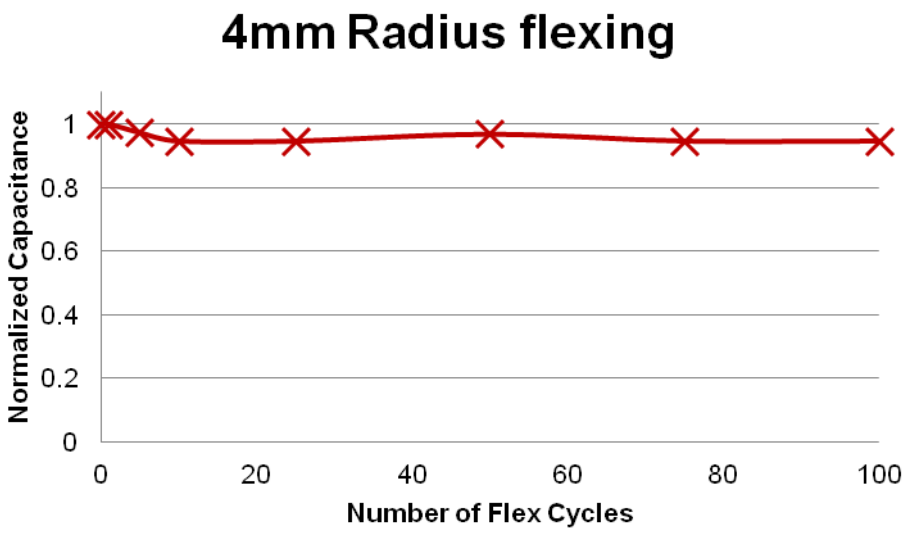

Fig. 14 Normalized capacitance of the capacitor in Fig. 9 after additional bending to a radius of 4 mm

4. Conclusions

We have demonstrated inkjet-printed, graphene-based, flexible packaged supercapacitors. Eventually, the metal current collector, graphene active electrode material, electrolyte, and separator will all be printed. However, inkjet printing has stringent ink requirements, which may make other printing technologies more attractive for printing metal current collectors and thick electrodes. The FEP sealing layer is not a mechanically stable substrate for the electrodes/current collectors, so these should be printed on bare Kapton or a gap should be left for heat sealing with a metal tab. The Kapton substrates used have a number of challenges including permeability and weak bond strength. In addition, while ionic liquid was well contained by Kapton; aqueous, propylene carbonate or acetonitrile electrolytes were not. Laminated packaging films are needed for increasing shelf life when using aqueous or organic electrolytes. The fully packaged device performance is low in these prototypes, in part due to the flat form factor, but there are a number of areas to optimize: package, current collector, electrode thickness, electrolyte, etc. An interdigitated electrode design may be desirable as it would simplify the packaging, eliminate the separator, and prevent the electrodes from pulling apart as the supercapacitor is bent. The degradation of ionic liquid based supercapacitors due to water permeation into the package also needs to be studied. A 6.9 mF in 3 x 3 cm package of 0.24 g demonstrated with BMIM BF_4 had an energy density of 5.5 Wh/kg measured at 0.25 A/g, and a power density of 19 kW/kg per mass of graphene measured at 10 A/g with the device tested to 3 V. The cycle life of the devices was improved through higher temperature thermal reduction of the electrodes. The capacitance retention as a function of bending was found to be excellent for these devices.

5. References

1. Pandolfo AG, Hollenkamp AF. J. Power Sources. 2006;157:11–27.
2. Le LT, Ervin MH, Qui H, Fuchs BE, Zunino J, Lee WY. in 11th IEEE Intl. Conf. on Nanotech., Portland, Oregon, 15–18 Aug 2011, pp. 67–71.
3. Davies A, Yu A. The Canadian J Chem. Engineering. 2011;89:1342–1356.
4. Le LT, Ervin MH, Qui H, Fuchs BE, Lee WY. Electrochem. Comm. 2011;13:355–358.
5. Cullis H. American Fluoroseal Corp., private communication, June 2012.
6. Stoller MD, Ruoff RS. Energy and Environ. Sci. 2010;3:1294–1301.
7. Burke A. Electrochimica Acta. 2007;53:1083–1091.
8. Liu P, Soukiazian S, Verbrugge M. J Power Sources. 2006;156:712–718.

List of Symbols, Abbreviations, and Acronyms

Au	gold
BMIM BF_4	1-butyl-3-methylimidazolium tetrafluoroborate
CO_2	carbon dioxide
CV	cyclic voltammetry
ESR	equivalent series resistance
FEP	fluorinated ethylene propylene
GO	graphene oxide
H_2SO_4	sulfuric acid
K_2SO_4	potassium sulfate
Kapton	DuPont trademarked polyimide film
KOH	potassium hydroxide
Li	lithium
rGO	reduced graphene oxide
Pt	platinum
SEM	scanning electron microscopy
Ti	titanium

1 (PDF)	DEFENSE TECH INFO CTR ATTN DTIC OCA
2 (PDF)	US ARMY RSRCH LABORATORY ATTN IMAL HRA MAIL & RECORDS MGMT ATTN RDRL CIO LL TECHL LIB
1 (PDF)	GOVT PRNTG OFC ATTN A MALHOTRA
1 (PDF)	US ARMY RSRCH LAB ATTN RDRL SER L M ERVIN

INTENTIONALLY LEFT BLANK.